

CLINICAL REPORT

A novel frameshift mutation of *DVL1*-induced Robinow syndrome: A case report and literature review

Ruolan Hu | Yu Qiu | Yifei Li  | Jinrong Li 

Key Laboratory of Birth Defects and Related Diseases of Women and Children of MOE, Department of Pediatrics, West China Second University Hospital, Sichuan University, Chengdu, China

Correspondence

Yifei Li and Jinrong Li, Department of Pediatrics, West China Second University Hospital, Sichuan University, No. 20, 3rd section, South Renmin Road, Chengdu 610041, China. Email: liyfwch@scu.edu.cn (Y. L.) and Email: lijnrong224@163.com (J. L.)

Funding information

Central Government Funds of Guiding Local Scientific and Technological Development for Sichuan Province, Grant/Award Number: 2021ZYD0105; National Natural Science Foundation of China, Grant/Award Number: 81700360; Technology Project of Sichuan Province of China, Grant/Award Number: 2020YFS0102

Abstract

Background: Robinow syndrome is a rare genetic disorder that affects the development of multiple systems. Due to its low prevalence and diversity of phenotypic presentation it has been challenging to definitively characterize features of Robinow syndrome.

Methods: We performed DNA extraction, whole-exome sequencing analysis, and mutation analysis of *DVL1* to obtain genetic data on the patient. We subsequently analyzed the patient's clinical and genetic data.

Results: The proband was a 3-month-old female infant who suffered from significant global developmental delay and metabolic disorder. The main clinical manifestations included facial dysmorphisms, bilateral dislocation of the hip joint, and hearing impairment. Whole-exome sequencing of the patient's DNA revealed a heterozygous mutation of c.1620delC in *DVL1*. Analysis with the MutationTaster application indicated that both were pathogenic (probability = 1), causing frameshift mutations affecting 107 amino acids (p.S542Vfs*107). Significant structural changes were identified in the amino acid sequence after the WNT signaling-related DEP domain site was predicted using the AlphaFold Protein structure database. The stability of the three main domains was then evaluated using SWISS-MODEL, and indicated that the mutation did not alter the DIX, PDZ, or DEP domain sequences. Because all reported pathogenic mutations were located near the DEP domain, we speculated that structural changes around the DEP domain may have impaired WNT domain function and WNT signaling, resulting in Robinow syndrome.

Conclusion: The present case suggests that molecular genetic screening is useful for the diagnosis of developmental disorders, particularly in children with a positive family history. In the current patient all the related pathological variants were located within a narrow locus. This report expands the known manifestations of Robinow syndrome and contributes to refinement of its molecular basis.

Ruolan Hu and Yu Qiu contributed equally to this work.

This is an open access article under the terms of the Creative Commons Attribution-NonCommercial-NoDerivs License, which permits use and distribution in any medium, provided the original work is properly cited, the use is non-commercial and no modifications or adaptations are made.

© 2022 The Authors. *Molecular Genetics & Genomic Medicine* published by Wiley Periodicals LLC.

KEYWORDS

case report, DVL1, genomic sequence, Robinow syndrome, WNT signaling deficiency

1 | BACKGROUND

Robinow syndrome was first described by Robinow et al. (1969), and is a genetically heterogeneous skeletal dysplasia caused by variations in a series of genes including receptor tyrosine kinase-like orphan receptor 2 (ROR2), WNT family member 5A (WNT5A), nucleoredoxin (NXN), Frizzled class receptor 2 (FZD2), DVL1, and DVL3 (Kirat et al., 2020; White et al., 2018), which are considered to participate in the non-canonical, β -catenin-independent signaling cascade. Facial features have been described as resembling those of a fetus, with a bulging frontal area of the skull, increased orbital distance, a wide mouth, and a small nose. Gingival hyperplasia and mesomelic limb shortening are infrequent abnormalities. Additional abnormalities including a small penis in males, hydronephrosis, orofacial clefts, and spine malsegmentation are also observed in some patients. Abnormalities including brachydactyly with a small hand for age, abnormal metacarpophalangeal pattern profile with the distal phalanges of the third and fourth digits less affected than the second and fifth, the first proximal phalanx shorter than the first metacarpal, and a short fifth middle phalanx with or without clinodactyly are considered the main clinical presentations of Robinow syndrome, and provide cues for its diagnosis (Kaissi et al., 2020). These growth retardations and malformations strongly affect the lives of patients, and are associated with morbidity (Gerber et al., 2020).

Although using whole-exome sequencing (WES) and 3D ultrasound could help to reach a diagnosis of Robinow syndrome during pregnancy (Jeppesen et al., 2017; Yang et al., 2020). But most of the cases could only receive an accurate diagnosis postnatally as the features of Robinow syndrome overlap with those of some other malformation syndromes (Castro et al., 2014). There is an urgent need to find an accurate and efficient method to address Robinow syndrome at an early age. Only a few case reports have described onset in patients with Robinow syndrome (Qaiser et al., 2009). Generally such syndromes lack specific clinical manifestations, rendering accurate discrimination between a series of genetic syndromes associated with global developmental retardation difficult. With the rapid development of whole-exome WES technology, a set of genetic mutations have been demonstrated to reveal the true causes of developmental disorders such as Robinow syndrome. Herein, we describe the case of young age onset Robinow syndrome reported in literature.

Initial presentation was due to bilateral dislocation of the hip joint and hearing impairment induced by an unreported mutation site in DVL1. Bilateral dislocation of the hip joint is a newly identified onset symptom of Robinow syndrome, which in the present case facilitated accurate diagnosis at the very young age of 3 months. Below we describe the role of WES in the diagnosis of Robinow syndrome in the current patient, and discuss the molecular function of the DVL1 protein.

2 | METHODS

2.1 | Ethical compliance

The study was approved by the ethics committee of the West China Second Hospital of Sichuan University (approval no. 2014-034). We obtained written, informed consent from the patient's parents prior to performing WES and for the inclusion of the patient's clinical and imaging details in publications.

2.2 | DNA extraction and WES analysis

A peripheral blood sample was obtained from the patient in an ethylenediaminetetraacetic acid (EDTA) anticoagulant blood sample tube that stored at 4°C for less than 6 hr. DNA was extracted using the Blood Genome Column Medium Extraction Kit (Tiangen Biotech, Beijing, China) according to the manufacturer's instructions. Protein-coding exome enrichment was performed using the xGen Exome Research Panel v1.0, comprising 429,826 individually synthesized and quality-controlled probes targeting 49.11 Mb of protein-coding region (>23,000 genes) of the human genome. WES was performed using the NovaSeq 6000 platform (Illumina, San Diego, CA, USA), and the raw data were processed using FastP to remove adapters and filter low-quality reads. Paired-end reads were aligned to the Ensembl GRCh38/hg38 reference genome using the Burrows-Wheeler Aligner. Variant annotation was performed in accordance with database-sourced minor allele frequencies (MAFs) and practical guidelines on pathogenicity issued by the American College of Medical Genetics. The annotation of MAFs was performed based on the 1000 Genomes, dbSNP, ESP, ExAC, and Chigene in-house MAF database, Provean, Sift, Polyphen2_hdiv,

and Polypen2_hvar databases using R software (R Foundation for Statistical Computing, Vienna, Austria). The sequencing data have been deposited in GSA database (<http://ngdc.cncb.ac.cn/gsub/>) (HRA001665).

2.3 | Mutation analysis of *DVL1*

To elucidate the molecular architecture of the human *DVL1* gene, we used MutationTaster with R software to predict the pathogenicity of *DVL1* c.1620delC and assess the impact of these mutations on protein structure. As there is no available protein crystal structure for *DVL1*, AlphaFold protein structure database (<https://alphafold.ebi.ac.uk/>) tool has been used to predicted protein crystal structure. The protein structure of *DVL1* has been built and named AF-P51141-F1 (Jumper et al., 2021; Tunyasuvunakool et al., 2021). Within the structure, three important domains have been revealed with analyzed crystal structure. Then we performed modeling analysis using the SWISS-MODEL (<https://swissmodel.expasy.org/>) for the three domains with the 3pz8.1.A, 6lca.1.A, and 1fsh.1.A template. We estimated the capability of the protein structure using Ramachandran plots. The signature vector that was ultimately generated was used to train the predictive classification and regression model for calculating the change in Gibbs folding free energy ($\Delta\Delta G$) induced by the mutations.

3 | RESULTS

3.1 | History of illness and physical examination

The proband was a 3-month-old male infant who was admitted to hospital due to facial dysmorphisms. Gestational ultrasound had detected abnormal bone development, but a panel of DNA high-pass sequencing failed to identify any abnormalities associated with chondroplasia. The patient was delivered at 39 gestational weeks by cesarean section, with an Apgar score of 10 at 1, 5, and 10-min timepoints. Postnatal jaundice was slightly increased 5 days after birth (total bilirubin 231.6 $\mu\text{mol/L}$ [13.5 mg/dl], direct bilirubin 10.9 $\mu\text{mol/L}$, indirect bilirubin 220.7 $\mu\text{mol/L}$), and subsided spontaneously. No repeated respiratory infections or other diseases occurred. The birth weight of the child was 3100 g, and her height was 50 cm.

The patient exhibited abnormal facial features and significant developmental delay, including a protruding forehead, wide eye distance (2.3 ± 0.4 cm at the age of 3 months), collapsed nose bridge, thick upper lip, mildly

high palatal arch, abnormal alveolar dysplasia, curled tragus, and slightly lower ear position (two-ear spiral slightly lower than two-eye level) (Figure 1a). Limited hip extension of both lower extremities was evident (Figure 1b). She exhibited global developmental retardation (weight at 3 months 5200 g, Z-score -1.49 , height at 3 months 56 cm, Z-score -2.36). Postnatally the average monthly increase in weight was 0.7 kg and the average monthly increase in height was 2 cm. There was no significant difficulty in milk feeding, and the estimated energy supplementation was considered basically sufficient. His parents reported that the he exhibited disorder in trancing particles and sounds. Bayley Scales of Infant and Toddler Development indicated substantial developmental retardation at the age of 2 months and 1 day ($< 0.1\%$ percentile). Besides, any potential poisoning or radiological exposure had been excluded.

3.2 | Laboratory and radiology results

Blood gas analysis indicated high carboxyhemoglobin of 1.90 (normal range [NR] 0.5–1.5). The results of blood biochemical tests indicated low levels of ALT (68 U/L, NR < 49 U/L), AST (69 U/L, NR < 40 U/L), lactate dehydrogenase (302 U/L, NR 120–246 U/L), and creatinine (17 $\mu\text{mol/L}$, NR 17.3–54.6 $\mu\text{mol/L}$). A low serum level of total vitamin D of 23.8 ng/mL (NR 30–100 ng/mL) indicated vitamin D deficiency. Several tests were conducted to investigate potential reasons for the growth retardation, the results of which included β -propionic butyric acid 0.15 mmol/L (NR 0–0.27 mmol/L), pyruvate 59.90 $\mu\text{mol/L}$ (NR 20–100 $\mu\text{mol/L}$), lactase 2.28 mmol/L (NR 0.5–2.2 mmol/L), IGF1 28.30 ng/mL (NR 51–327 ng/mL), IGFBP3 1.23 $\mu\text{g/mL}$ (NR 0.7–3.9 $\mu\text{g/mL}$), TSH 2.627 mIU/L (NR 0.64–6.27 mIU/L), FT3 5.33 pmol/L (NR 5.1–8.0 pmol/L), FT4 13.15 pmol/L (NR 12.26–21.67 pmol/L), alkaline phosphatase 182 U/L, P 2.02 mmol/L, and Ca^{2+} 2.26 mmol/L. Tandem mass spectrometry was used to measure metabolic status, and general disorder of almost all parameters was identified (Table S1).

Radiology results indicated that the patient had dislocated hip joints on both sides (Figure 1c), and that it was more pronounced on the left side. The radius was shortened on both sides (Figure 1c–e), the thumbs and fifth phalanxes of both hands were curved, the fifth distal phalanx on the left was slightly bifurcated (Figure 1d), and the thoracic and lumbar vertebrae were kyphotic with the thoracic 12 vertebrae as the center (Figure 1f). Echocardiography indicated ductus arteriosus. Brain magnetic resonance imaging revealed change of form of her lateral ventricles on both sides, and thinning of the corpus callosum.



FIGURE 1 Clinical and radiology manifestation in the current proband. (a) The patient exhibited abnormal facial features and significant developmental delay, including a protruding forehead, wide eye distance, collapsed nose bridge, thick upper lip, mildly high palatal arch, abnormal alveolar dysplasia, curled tragus, and slightly lower ear position (two-ear spiral slightly lower than two-eye level). (b) Limited hip extension of both lower extremities was evident. (c) Radiology results indicated that the patient had dislocated hip joints on both sides. (d and e) The radius was shortened on both sides. And the thumbs and fifth phalanges of both hands were curved, the fifth distal phalanx on the left was slightly bifurcated. (f) The thoracic and lumbar vertebrae were kyphotic with the thoracic 12 vertebrae as the center

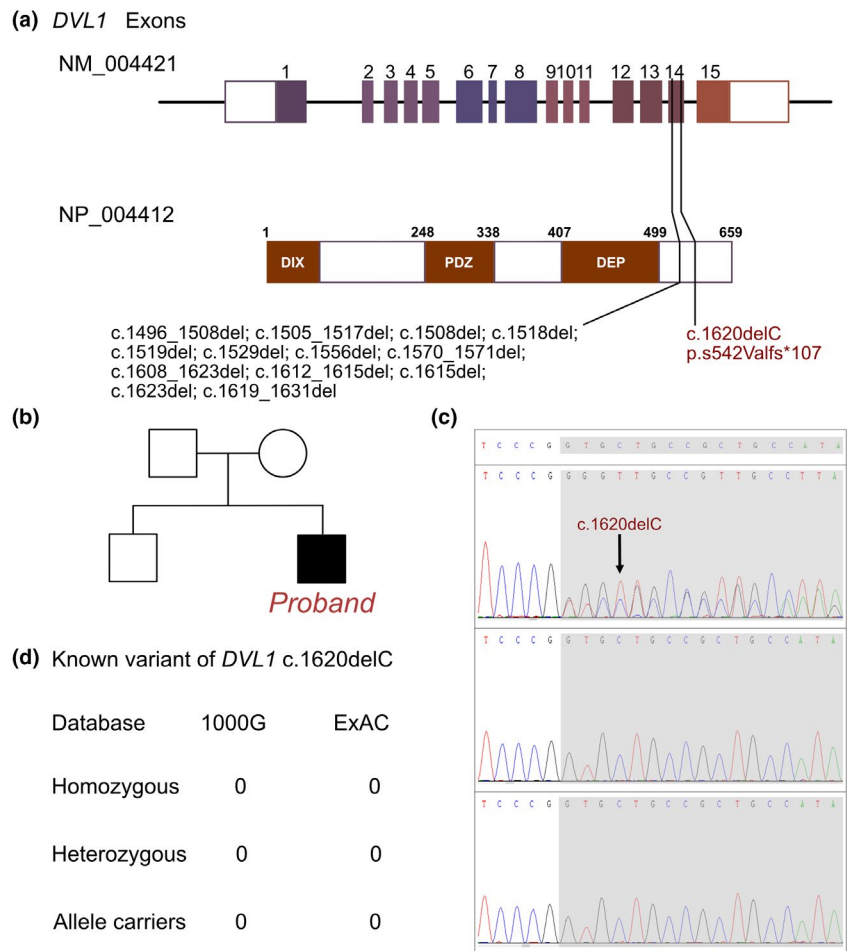
3.3 | Molecular results

Based on the clinical manifestations and laboratory analyses, a genetic disorder was strongly suspected. WES was performed using the Illumina NovaSeq 6000 platform, and identified a de novo c.1620delC (p.S542Vfs*107) heterozygous mutation in the *DVL1* gene. The patient's mother and father were both absent from this site (Figure 2b,c). The other relatives of this patients did not present similar clinical manifestation. This mutation should be treated as an accidental or *de novo* one. According to the American College of Medical Genetics, these variants have uncertain pathogenicity (PVS1_Moderate+PS2 + PM2_Supporting). c.1620delC has not been reported in any populations; this is the first report of this variant (Figure 2d). Analysis performed with MutationTaster revealed that this mutation

is considered pathogenic due to amino acid sequence changes, frameshift, protein features affected, and truncated proteins (probability = 1 for c.1620delC).

AlphaFold was used to predict the protein structure of *DVL1*, and the truncated sequence site of the protein was labeled (Figure 3a). Although the predicted protein covered the entire length of the amino acid sequence, only three domains demonstrated high confidence in the crystal structure (pLDDT >70). Other parts demonstrated low confidence in the crystal structure. All potential templates were searched and only parts of the protein had been analyzed previously, so the AlphaFold-predicted structure was the only model that could be used. SWISS-MODEL was then used to predict the crystal structures of the variant's three domains (DIX, PDZ, and DEP) (Figure 3b–d). The stable structure at

FIGURE 2 The *DVL1* mutations in this family. (a) Summary of current reports on individual *DVL1* mutations. (b) Sanger sequencing validation of the current proband and his parents. (c) Family pedigree revealing the maternal carrier of *DVL1* c.1620delC (p.S542Vfs*107). The current proband exhibited severe developmental retardation with de novo heterozygous mutation of *DVL1* c.1620delC. (d) The prevalence of *DVL1* mutations of c.1620delC



the three domain sites was recorded. The DIX domain is most likely involved in regulating canonical WNT signaling, leading to β -catenin stability. The PDZ domain is required for *DVL1*-mediated microtubule stabilization. The DEP domain is predicted to be important for protein interaction and most likely has a role in signal transduction. All *DVL1* mutations were located in exon 14, indicating frameshift and a truncated protein structure following the DEP domain. Thus, we surmise that the altered amino acid sequence may have co-effects related to the DEP domain, and impair WNT signaling.

3.4 | Treatment and clinical outcome

Additional vitamin D was provided, and nutritional guidance was provided to strengthen supplementary energy and improve metabolic disorders. Rehabilitation training was provided to address neuromotor retardation and developmental delay. Careful and continuous follow-up and evaluation were then conducted. Developmental assessment should be performed every month in the infant phase and every 3 months after that, or more frequently as needed if cognitive delays are identified.

4 | DISCUSSION AND CONCLUSION

Robinow syndrome exhibits strong clinical and genetic heterogeneity. The clinical features identified in the current patient were characteristic of dysmorphic craniofacial features resembling a “fetal face”, mesomelic limb shortening, kyphoscoliosis, hemivertebrae, hypoplastic external genitalia, and renal anomalies (Patton & Afzal, 2002). Notably, some of the patient's symptoms were not concordant with the classic Robin's syndrome description, such as external genital abnormalities, hemivertebrae, and renal anomalies. Robin's syndrome was first described in patients with *WNT5A* mutations. Subsequent studies indicated the dominant role of the WNT pathway in cell fate determination, including cell proliferation, migration, and the maintenance of cellular planar polarity. Genes involved in WNT signal transduction have been identified as being associated with the onset of Robinow syndrome, as have *DVL1*, *DVL3*, *FZD2*, *NXN*, and *ROR2*. *WNT5A* reportedly functions as a mediator that interacts with *ROR2* and *FZD2*. The trans-membranous protein *FZD2* then transduces signals to *DVLs*, which may be inhibited by *NXN*. *DVL* molecules induce intracellular

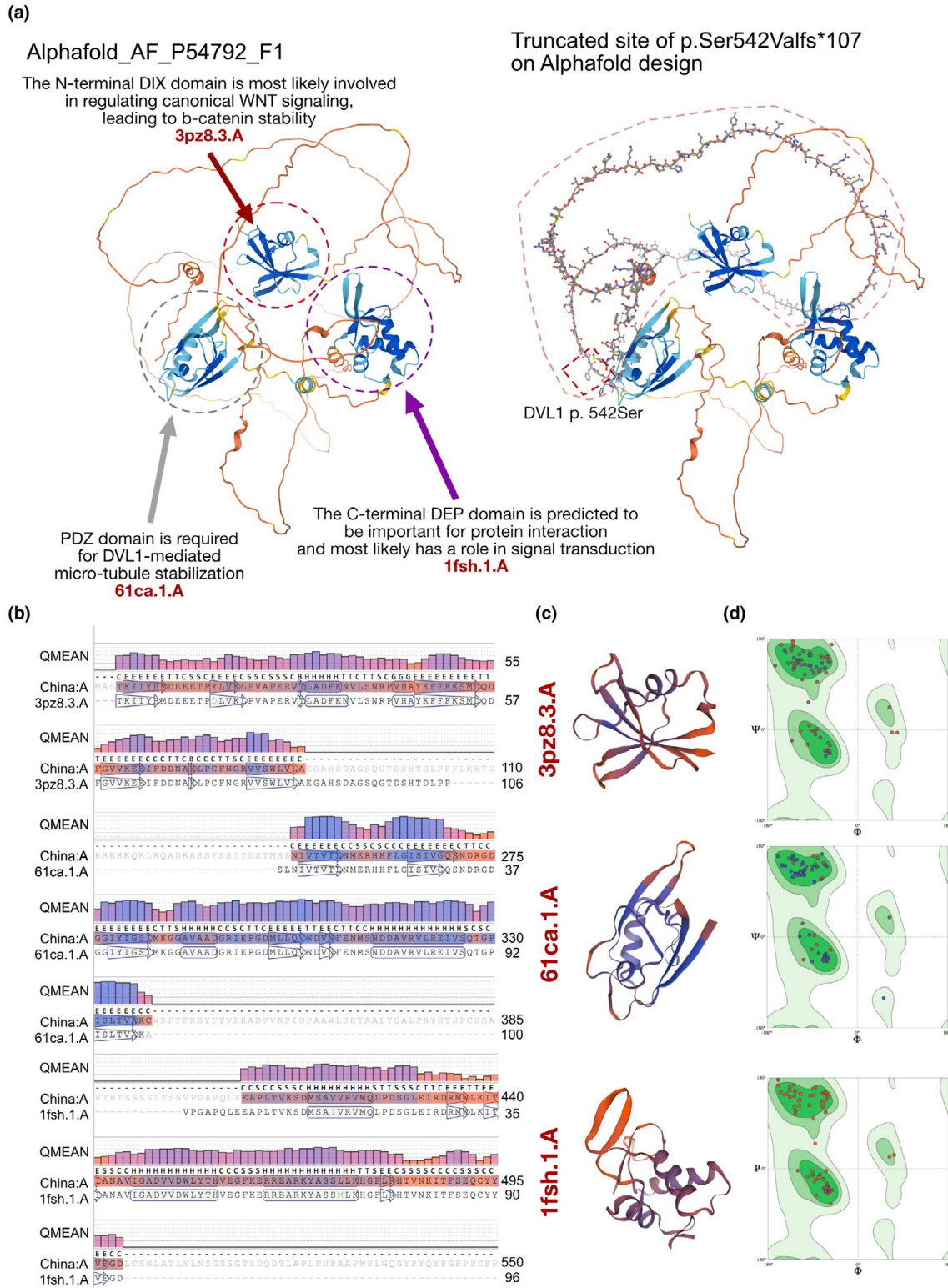


FIGURE 3 The effects of *DVL1* c.1620delC mutation on the molecular structure of the protein. (a) AlphaFold protein structure database used to predict the *DVL1* wild-type protein crystal structure. Changes in structure were identified with low confidence. Three important DEP domains were revealed that were clearly involved in WNT signal transduction. (b) Amino acid sequences in three functional domains that have been analyzed. (c) Individual crystal structures of functional domains according to the 3pz8.3.A, 61ca.1.A, and 1fsh.1.A model template. (d) Ramachandran plots of three functional domains in wild-type sequences

WNT/PCP signaling, but previous studies have revealed locus heterogeneity with rare variants among all the reported mutations (Zhang et al., 2020).

DVL is a segment polarity gene that was first identified in *Drosophila*. Decades ago studies indicated that the gene-mediated WNT/Wg signal transduction of patterning information in multiple tissues, mainly affecting the developmental process, including axial patterning of legs and wings of adult *Drosophila*. Three *DVL* homologs have been confirmed in humans, *DVL1*, *DVL2*, and *DVL3*, which share approximately 65% amino acid sequence identity. Mouse experiments suggest that *DVL* contributes to neurological and social behavior development. White et al. (J. White et al., 2015) described seven patients with *DVL1* mutations that induced frameshift resulting in Robinow syndrome. All were located in exon 14, which encodes the structure of the DEP domain. Zhang et al. (Zhang et al., 2020) also identified a *DVL1* mutation located in exon 14 that resulted in Robinow syndrome. A series of case reports from Mishra et al. (Mishra et al., 2020; Rai et al., 2021) and Rai et al. (Mishra et al., 2020; Rai et al., 2021) also described mutations at *DVL1* sites located in exon 14. To date, c.1496_1508del, c.1505_1517del, c.1508del, c.1518del, c.1519del, c.1529del, c.1556del, c.1570_1571del, c.1608_1623del, c.1612_1615del, c.1615del, c.1623del, and c.1619_1631del have been reported. Interestingly, no reported mutations have been located in DIX, PDZ, or DEP domains. All the retrieved variants identified and those in the present case were within a very narrow locus, from 1496 to 1631 bases. We hypothesize that this region is a key locus for establishing normal protein structure and maintaining the biological function of the DEP domain in WNT signal transduction. Notably however, there is no crystal protein structure model for the entire protein based on cryo-electron microscopy available. Thus, structure-based analysis is urgently required for this locus. In the current case the clinical manifestations were not typical, but the severe developmental delay prompted us to conduct a WES test. A likely pathogenic *DVL1* variant was identified which facilitated a diagnosis of Robinow syndrome based on the mutation site and protein structure assessments. *DVL1* pathogenic alleles are a specific risk factor for neurodevelopmental disability (Schwartz et al., 2020). Therefore, prompt diagnosis and treatment of Robinow syndrome is very important in order to improve the prognosis. Herein, we have described the youngest patient to be diagnosed with Robinow syndrome, and the novel mutation site c.1620delC which is also located in the region of interest, reflecting the importance of this region of interest in maintaining gene biological function.

In conclusion, above we have described the youngest patient with Robinow syndrome reported to date, who exhibited severe global developmental delay as well as

bilateral hip joint dislocation and hearing impairment. A *DVL1* variant (c.1620delC) was responsible for Robinow syndrome in this patient. WES is a very powerful and favorable technique for the diagnosis of Robinow syndrome, because a delayed diagnosis may result in morbidity. Currently no mutation has been identified within the three crucial domains (DIX, PDZ, and DEP) for WNT signal transduction. All the related pathologic variants were located in a narrow locus. The current report expands the manifestations of Robinow syndrome and contributes to the refinement of its molecular basis.

ACKNOWLEDGMENTS

This work was supported by grants from the National Natural Science Foundation of China (No. 81700360), Technology Project of Sichuan Province of China (2020YFS0102), and Central Government Funds of Guiding Local Scientific and Technological Development for Sichuan Province (2021ZYD0105).

CONFLICT OF INTEREST

The authors declare that they have no conflict of interest.

AUTHOR CONTRIBUTIONS

Ruolan Hu and Yu Qiu contributed equally to this work. Yifei Li and Jinrong Li were the patient's physicians. Ruolan Hu and Yu Qiu reviewed the literature and contributed to manuscript drafting; Yifei Li conceptualized and designed the study, coordinated and supervised data collection, and critically reviewed the manuscript for important intellectual content. Yu Qiu, Ruolan Hu, and Jinrong Li were responsible for the revision of the manuscript for important intellectual content; all authors issued final approval for the version to be submitted.

ETHICAL APPROVAL

This study was approved by the Ethics Committee of West China Second Hospital of Sichuan University (2014-034). And informed consent from the patient's parents prior to conducting the WES had been obtained, including the patient's clinical and imaging details in the manuscript for the purpose of publication.

CONSENT FOR PUBLICATION

The patient's parents provided written informed consent to the performance of WES, and the publication of this report.

DATA AVAILABILITY STATEMENT

The sequencing data have been deposited in GSA database (ngdc.cnbc.ac.cn/gsub/) (HRA001665). Other data sets used in this study are available from the corresponding author upon reasonable request.

ORCID

Yifei Li  <https://orcid.org/0000-0002-3096-4287>Jinrong Li  <https://orcid.org/0000-0003-1200-3842>

REFERENCES

- Castro, S., Peraza, E., Barraza, A., & Zapata, M. (2014). Prenatal diagnosis of Robinow syndrome: A case report. *Journal of Clinical Ultrasound*, *42*(5), 297–300. <https://doi.org/10.1002/jcu.22103>
- Gerber, J. A., Sheth, K. R., & Austin, P. F. (2020). Robinow syndrome: Genital analysis, genetic heterogeneity, and associated psychological impact. *American Journal of Medical Genetics. Part A*, *185*, 3601–3605. <https://doi.org/10.1002/ajmg.a.61981>
- Jeppesen, B. F., Hove, H. B., Kreiborg, S., Hermann, N. V., Darvann, T. A., & Jørgensen, F. S. (2017). Prenatal diagnosis of autosomal recessive Robinow syndrome using 3D ultrasound. *Clin Case Rep*, *5*(7), 1072–1076. <https://doi.org/10.1002/ccr3.784>
- Jumper, J., Evans, R., Pritzel, A., Green, T., Figurnov, M., Ronneberger, O., Tunyasuvunakool, K., Bates, R., Židek, A., Potapenko, A., & Bridgland, A. (2021). Highly accurate protein structure prediction with AlphaFold. *Nature*, *596*, 583–589. <https://doi.org/10.1038/s41586-021-03819-2>
- Kaissi, A. A., Kenis, V., Shboul, M., Grill, F., Ganger, R., & Kircher, S. G. (2020). Tomographic study of the malformation complex in correlation with the genotype in patients with Robinow syndrome: Review article. *Journal of Investigative Medicine High Impact Case Reports*, *8*, 232470962091177. <https://doi.org/10.1177/2324709620911771>
- Kirat, E., Mutlu Albayrak, H., Sahinoglu, B., Gurler, A. I., & Karaer, K. (2020). Autosomal recessive Robinow syndrome with novel ROR2 variants: Distinct cases exhibiting the clinical variability. *Clinical Dysmorphology*, *29*(3), 137–140. <https://doi.org/10.1097/mcd.0000000000000319>
- Mishra, R., Jain, V., Gupta, D., Saxena, R., Kulshreshtha, S., Ramprasad, V. L., Verma, I. C., & Dua Puri, R. (2020). Robinow syndrome and brachydactyly: An interplay of high-throughput sequencing and deep phenotyping in a kindred. *Molecular Syndromology*, *11*(1), 43–49. <https://doi.org/10.1159/000505506>
- Patton, M. A., & Afzal, A. R. (2002). Robinow syndrome. *Journal of Medical Genetics*, *39*(5), 305–310. <https://doi.org/10.1136/jmg.39.5.305>
- Qaiser, R., Scott, R. M., & Smith, E. R. (2009). Identification of an association between Robinow syndrome and moyamoya. *Pediatric Neurosurgery*, *45*(1), 69–72. <https://doi.org/10.1159/000204907>
- Rai, A., Patil, S. J., Srivastava, P., Gaurishankar, K., & Phadke, S. R. (2021). Clinical and molecular characterization of four patients with Robinow syndrome from different families. *American Journal of Medical Genetics. Part A*, *185*(4), 1105–1112. <https://doi.org/10.1002/ajmg.a.62082>
- Robinow, M., Silverman, F. N., & Smith, H. D. (1969). A newly recognized dwarfing syndrome. *American Journal of Diseases of Children*, *117*(6), 645–651. <https://doi.org/10.1001/archpedi.1969.02100030647005>
- Schwartz, D. D., Fein, R. H., Carvalho, C. M. B., Sutton, V. R., Mazzeu, J. F., & Axelrad, M. E. (2020). Neurocognitive, adaptive, and psychosocial functioning in individuals with Robinow syndrome. *American Journal of Medical Genetics. Part A*, *185*, 3576–3583. <https://doi.org/10.1002/ajmg.a.61854>
- Tunyasuvunakool, K., Adler, J., Wu, Z., Green, T., Zielinski, M., Židek, A., Bridgland, A., Cowie, A., Meyer, C., Laydon, A., Velankar, S., Kleywegt, G. J., Bateman, A., Evans, R., Pritzel, A., Figurnov, M., Ronneberger, O., Bates, R., Kohl, S. A. A., ... Hassabis, D. (2021). Highly accurate protein structure prediction for the human proteome. *Nature*, *596*, 590–596. <https://doi.org/10.1038/s41586-021-03828-1>
- White, J., Mazzeu, J. F., Hoischen, A., Jhangiani, S. N., Gambin, T., Alcino, M. C., Penney, S., Saraiva, J. M., Hove, H., Skovby, F., Kayserili, H., Estrella, E., Vulto-van Silfhout, A., Steehouwer, M., Muzny, D. M., Sutton, V. R., Gibbs, R. A., Baylor-Hopkins Center for Mendelian Genomics, Lupski, J. R., ... Carvalho, C. M. (2015). DVL1 frameshift mutations clustering in the penultimate exon cause autosomal-dominant Robinow syndrome. *American Journal of Human Genetics*, *96*(4), 612–622. <https://doi.org/10.1016/j.ajhg.2015.02.015>
- White, J. J., Mazzeu, J. F., Coban-Akdemir, Z., Bayram, Y., Bahrambeigi, V., Hoischen, A., Van Bon, B., Gezdirici, A., Gulec, E. Y., Ramond, F., Touraine, R., Thevenon, J., Shinawi, M., Beaver, E., Heeley, J., Hoover-Fong, J., Durmaz, C. D., Karabulut, H. G., Marzioglu-Ozdemir, E., ... Carvalho, C. M. B. (2018). WNT signaling perturbations underlie the genetic heterogeneity of Robinow syndrome. *American Journal of Human Genetics*, *102*(1), 27–43. <https://doi.org/10.1016/j.ajhg.2017.10.002>
- Yang, K., Zhu, J., Tan, Y., Sun, X., Zhao, H., Tang, G., Zhang, D., & Qi, H. (2020). Whole-exome sequencing identified compound heterozygous variants in ROR2 gene in a fetus with Robinow syndrome. *Journal of Clinical Laboratory Analysis*, *34*(2), e23074. <https://doi.org/10.1002/jcla.23074>
- Zhang, C., Mazzeu, J. F., Eisfeldt, J., Grochowski, C. M., White, J., Akdemir, Z. C., Jhangiani, S. N., Muzny, D. M., Gibbs, R. A., Lindstrand, A., Lupski, J. R., Sutton, V. R., & Carvalho, C. M. B. (2021). Novel pathogenic genomic variants leading to autosomal dominant and recessive Robinow syndrome. *American Journal of Medical Genetics. Part A*, *185*, 3593–3600. <https://doi.org/10.1002/ajmg.a.61908>

SUPPORTING INFORMATION

Additional supporting information may be found in the online version of the article at the publisher's website.

How to cite this article: Hu, R., Qiu, Y., Li, Y., & Li, J. (2022). A novel frameshift mutation of *DVL1*-induced Robinow syndrome: A case report and literature review. *Molecular Genetics & Genomic Medicine*, *10*, e1886. <https://doi.org/10.1002/mgg3.1886>